

Reducing the Number of Receiving Channels Using Transmit-receive Symmetry in Synthetic Transmit Aperture Imaging

Ying Li, Ping Gong, Michael C. Kolios, Yuan Xu

Physics Department
Ryerson University
Toronto, Canada
yxu@ryerson.ca

Abstract—Synthetic transmit aperture (STA) imaging has been widely studied in ultrasound imaging. Usually the number of receiving channels is the same as the number of the array elements (N). When the number of receiving channels is large, such as the matrix array for 3D imaging, the system cost will be high due to the receiving electronics for each element. Therefore, it is desirable to reduce the number of receiving channels while keeping a large number of transmit channels. In this paper, we studied with Field II Hadamard-encoded synthetic transmit aperture imaging systems with about $N/2$, $N/4$ and $N/8$ receiving channels. There were N Hadamard-encoded transmission events for one frame of image. The pseudoinverse was applied to the acquired RF data to estimate the equivalent signal in the traditional STA. We found that applying the transmit-receive symmetry of RF signals can reduce the receiving channels by half without compromising image quality. We also compared different methods to encode the receivers when the receiving channels were reduced to about $N/4$ and $N/8$.

Keywords—Hadamard encoding, sparse array, pseudoinverse, encode receiver

I. INTRODUCTION

One major limitation of synthetic transmit aperture (STA) is the loss in the SNR of RF data because only one or a few elements are used in each transmission. Hadamard matrix has been proposed to encode either the amplitude [1] or the delay [2] of transmissions to improve the SNR in STA. Generally, multiple elements can be coded according to the Hadamard matrix to fire simultaneously to increase the transmitted power.

In STA, the probe array has a fixed number of elements, which are usually stationary [3]. The number of receiving channels of an ultrasound imaging system is usually the same as the number of array elements. However, to generate a 3D ultrasound image, the 2D transducer array is usually required. Meanwhile, to avoid the grating lobes, the pitch of the array has to be less than half a wavelength [4]. When the number of receiving channels is large, the cost of the hardware system will be prohibitively high due to the electronics associated with the receiving channels for each element [5]. Therefore, many innovations in designing the effective sparse array have been

investigated in [6-12]. However, the quality of images cannot be preserved due to the reduction of the number of elements. There are grating lobes when using a periodic sparse array, while random sparse arrays suffer from the significant side lobes [13].

In this paper, we propose a method to spatially encode the transmission with Hadamard matrix to improve SNR and to encode the receiving element by combining the receiver elements. The transmit-receive symmetry property of the RF channel data was also used to solve for the equivalent signal in the traditional STA. A triangle pattern was designed to reduce the number of receiving channels for each transmission event. Then, pseudoinverse was used to decode the acquired RF signals to obtain the equivalent traditional STA data. The reconstructed results from this method have better contrast-to-noise ratio (CNR) compared to the periodic sparse array.

In section II, the theory of proposed method will be presented. Then the simulation parameters and implementations will be shown. The image quality metrics will be presented and applied to the images. In section III, the simulation results will be shown, the imaging quality of images generated with our proposed method will be assessed and compared with periodic sparse array methods. The discussion and conclusion will be shown in section IV.

II. METHODS

A. Encoding Operator

Assume the probe array has N elements. In the transmission process, we apply Hadamard matrix as the encoding matrix. To form one frame of image, there are L transmissions, in each of which the same N transmission elements are used. Therefore, an L -by- N Hadamard matrix \mathbf{T} can be formed. In the receiving mode, K receiving channels can be used for each transmission. We assume $L=N$ in this paper.

The encoding process can be described for each $l=1:L$ of the L transmission events as

$$\mathbf{T}_l \mathbf{S}(t) \mathbf{R}_l = \mathbf{m}_l(t) \quad (1)$$

where $\mathbf{S}(t)$ is equivalent traditional STA signal matrix, with a size N by N , ($S_{ij}(t)$ is the signal at t received by the j -th element when the i -th element transmits). $\mathbf{m}_l(t)$ is a measurement row vector of size K acquired from the selected output channels at time t in the l -th transmission event; \mathbf{T}_l is a row vector of size N to encode the transmission, and \mathbf{R}_l (N by K) is a matrix to encode the receiving elements. Notice that \mathbf{T} and \mathbf{R} can vary among different transmission events.

The transmission and receiving encoding process could be combined as a Kronecker product via a mathematical identity [14]. Therefore, an encoding operator can be defined as

$$\mathbf{E}_l = \mathbf{R}_l^T \otimes \mathbf{T}_l \quad (2)$$

where the superscript T means the transpose of the matrix. Thus, this encoding operator can be applied to STA signal. Note that to apply this operator properly, the traditional STA signal $\mathbf{S}(t)$ has to be vectorized into a column vector $\mathbf{S}_{vector}(t)$ by stacking the columns of \mathbf{S} . We have

$$\mathbf{E}_l \mathbf{S}_{vector}(t) = \mathbf{m}_l^T(t), l = 1:L \quad (3)$$

In addition, in standard STA the signal received at the i -th receiver and transmitted by the j -th transmitter is equivalent to the signal received at the j -th receiver and transmitted by the i -th transmitter, $S_{ij}=S_{ji}$. Eq. 3 for all the L transmission events plus the equations on the transmit-receive symmetry property will form a linear equation set. To recover \mathbf{S} from $\mathbf{m}_l^T(t)$, pseudo-inversion with regularization was used in the simulations.

There are $N(N-1)/2$ symmetry equations, and N^2 unknowns for one set of traditional STA data, therefore in principle $(N/2+1)$ receiving channels with N transmissions should be sufficient to recover the traditional STA data. In this paper, we chose $(N/2+1)$ receiving channels for each transmission according to the following triangle pattern.

B. The triangle pattern to select $N/2+1$ receiving elements

Here we first introduce a triangle pattern (patches A, B, and C in Fig. 1b), which was used to specify the $N/2+1$ receiving elements in each of the N Hadamard-encoded transmissions to obtain one frame of image. The vertical axis represents the index of a transmission event and the horizontal axis represents the index of all the receiving elements used in a transmission event. For example, any point inside a patch, (n_x, n_y) , means the n_x -th receiver is used in the n_y -th transmission. When $n_y \leq N/2$, the receiving elements include $1:n_y$ and $(N/2+n_y):N$; when $n_y > N/2$, the receiving elements include $1:N/2+1$. According to this method, the total number of output elements selected is $N/2+1$.

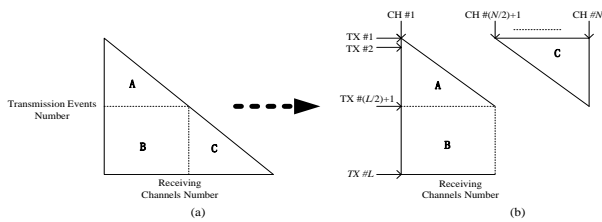


Fig. 1. Triangle pattern. (a) Original triangle pattern (b) transformed triangle pattern

C. Encoding scheme for $N/4+1$ receiving channels

In quarter receiving mode, two adjacent elements are combined together as one receiver (e.g. the first bundle includes the 1st and 2nd element). This will reduce the receiving channels to $N/2$ bundled elements. There are two sets of transmission and receiving encoding protocols to obtain one frame of image. In the first set, the $(2n-1)$ -th rows of N -th order Hadamard matrix are used to encode the transmissions, where $n=1:N/2$. So $N/2$ transmission events are used in the first set. The quarter-receiving encoding matrix $\mathbf{R}_{1/4}$ for all the $N/2$ transmission events is

$$\mathbf{R}_{1/4} = \mathbf{I}_{N/2} \otimes \mathbf{V}_2 \quad (4)$$

where \mathbf{I} is the identity matrix with the size of $N/2$ and \mathbf{V}_2 is a column vector of $(1, 1)$. Then we chose $N/4+1$ paired elements according to the triangle pattern to reduce the receiving channels further by half. Therefore, the final number of receiving channel is $N/4+1$. The second set of transmission and receiving encoding protocol is the same as the first set except that the $(2n)$ -th rows of N -th order Hadamard matrix are used to encode the transmissions, where $n = 1:N/2$.

D. Encoding scheme for $N/8+1$ receiving channels

This mode is similar to the quarter-receiving mode except that four adjacent elements in the receiver array are combined together as one receiver. For example, the first bundle includes the first four elements. The next bundle includes the fifth element to the eighth element, and so on. Four sets of transmission and receiving encoding protocols are used to obtain one frame of image. This will reduce the receiving channel number to $N/4$. In the first set the $(4n-3)$ -th rows of a N -th order Hadamard matrix are used to encode the transmissions, where $n = 1:N/4$. So there are $N/4$ transmission events in the first set. In each transmission of the first set, the receiving encoding matrix $\mathbf{R}_{1/8}$ for the first set is

$$\mathbf{R}_{1/8} = \mathbf{I}_{N/4} \otimes \mathbf{V}_4 \quad (5)$$

where \mathbf{I} is the identity matrix with the size of $N/4$, and \mathbf{V}_4 is a column vector of $(1, 1, 1, 1)$. After selecting $N/8+1$ from the $N/4$ receivers according to the triangle pattern, we can reduce the receiving channels further by half. Therefore, the final number of receiving channels is $N/8+1$. The second set of transmission and receiving encoding protocol is the same as the first set except that the $(4n-1)$ -th rows of N -th order Hadamard matrix are used to encode the transmissions, where $n = 1:N/4$.

The third and fourth set of transmission and receiving encoding protocol are similar to the first and second sets except that \mathbf{V}_4 is modified to a column vector of $(1, 1, -1, -1)$ as \mathbf{V}_4^M in the receiving-encoding scheme. Then, we have for the third and fourth set

$$\mathbf{R}_{1/8} = \mathbf{I}_{N/4} \otimes \mathbf{V}_4^M \quad (6)$$

In conclusion, the four sets of protocols will form a complete imaging protocol, in which, there are N transmissions and $(N/8+1)$ receiving channels in each transmission.

E. Methods in simulations

1) Simulation parameters

FIELD II program [15] was used to generate standard STA RF data. The probe was simulated as a 128-element, 2-cm wide, 5-MHz central frequency phased array with a 0.15-mm pitch, 0.01-mm kerf and 10-mm height. The sampling frequency was 40 MHz.

2) Simulation phantoms

There were two simulated phantoms in our simulations. The size of the first medium is 2 cm × 1 cm × 2 cm (Azimuth × Elevational × Axial), which contains five point targets placed at 4 mm apart from 7 mm to 23 mm depth. Another simulated phantom has the same size as the first medium, but with nine 4-mm-diameter hypo-echoic inclusions placed in three rows from top to bottom, and the centers are at 1 cm, 1.5 cm, and 2 cm depth, respectively. For each row, the centers of the three hypo-echoic lesions are separate by 6 mm apart horizontally. Eight point targets are included at two columns, four for each column. In each column, the point targets are placed at the depth of 0.75 mm, 1.35 mm, 1.75 mm, and 2.35 mm. The log-enveloped beamformed images were displayed after applying Hilbert transform and the logarithm compression.

F. Imaging quality metrics

Contrast-noise-ratio (CNR)

The CNR of inclusions was calculated as:

$$\text{CNR} = \frac{\mu_{\text{lesion}} - \mu_{\text{background}}}{\sqrt{\sigma_{\text{lesion}}^2 + \sigma_{\text{background}}^2}} \quad (7)$$

where μ_{lesion} and $\mu_{\text{background}}$ are the mean value of log-enveloped region of lesion and background respectively, and σ_{lesion} and $\sigma_{\text{background}}$ are the standard deviation of the log-enveloped region of the lesion and background, respectively.

III. RESULTS

Fig. 2 exhibits a) the log-enveloped image of the standard STA and b) the proposed method with symmetry property and 65 receiving channels selected according to the triangle pattern presented in II.B for each transmission. Fig. 2(c) shows the image without taking into account of the symmetry property

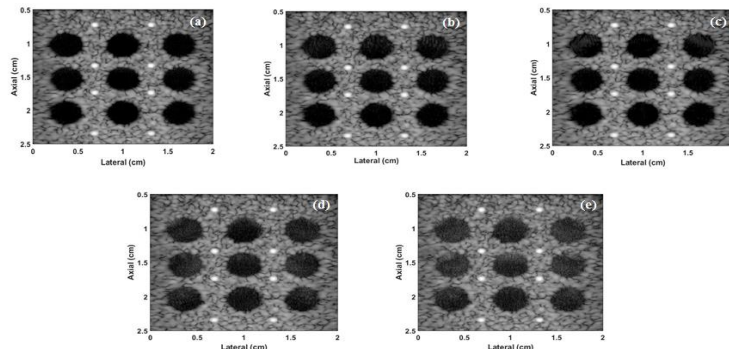


Fig. 4. Log-enveloped beamformed simulated images from (a) standard STA, (b) proposed method with 33 receiving channels, (c) proposed method with 17 receiving channels, (d) STA with 32 periodic-selected receiving elements (elements $4n-3$, where $n=1:N/4$), and (e) STA with 16 periodic-selected receiving elements (elements $8n-7$, where $n=1:N/8$). The image dynamic range is 65 dB.

but still using the same 65 selected receiving channels as in (b). The results illustrate that without using symmetry property, the image quality is severely degraded by the strong artifacts. This is also confirmed by the line-plots (Fig. 3) through the center of the point target at the center of the images. The line plot from the model with $N/2+1$ receivers and the symmetry property equations is almost identical to that from the standard STA imaging approach.

Fig. 4 shows the log-enveloped image from the second simulated phantom using (a) the standard STA approach, (b) our proposed method with 33 receiving channels for each transmission, (c) our proposed method with 17 receiving channels for each transmission, (d) STA with 32 periodic-selected receiving elements (elements $4n-3$, where $n=1:N/4$), and (e) STA with 16 periodic-selected receiving elements (elements $8n-7$, where $n=1:N/8$). As seen in Table 1, the CNR values of the lesions in the images from the proposed method are better than those from the model with periodically selected receiver elements.

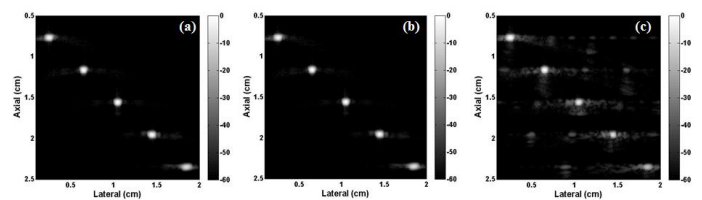


Fig. 2. Log-enveloped beamformed simulated images from (a) standard STA, (b) our proposed method with symmetry property and 65 receiving channels selected according to the triangle pattern for each transmission and (c) the method without symmetry property but with the same 65 selected receiving channels.

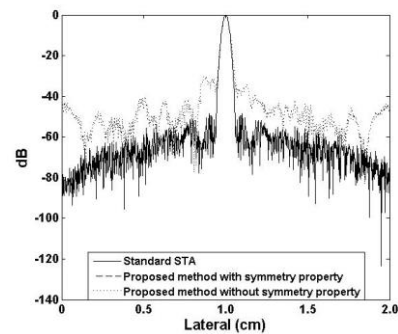


Fig. 3. Line-plot comparisons through the center of the point target at the center of the images between standard STA, our proposed method with symmetry property and the method without symmetry property.

TABLE I. CNR measurements of nine hypo-echoic inclusions in the images of (a) standard STA, (b) our proposed method with 33 receiving channels, (c) our proposed method with 17 receiving channels, (d) STA with 32 periodic-selected receiving elements, and (e) STA with 16 periodic-selected receiving elements.

Method	1-cm hypo lesions			1.5-cm hypo lesions			2-cm hypo lesions		
	Left	Middle	Right	Left	Middle	Right	Left	Middle	Right
Standard STA	-4.0714	-4.2016	-3.7896	-4.1168	-4.7093	-3.8033	-4.1198	-4.3769	-3.9540
Proposed (33)	-3.0883	-2.9962	-2.6495	-3.7994	-4.1432	-3.3892	-3.9020	-3.9381	-3.7152
Proposed (17)	-2.7089	-3.6930	-2.6684	-4.0467	-4.4955	-3.7181	-4.0432	-3.9763	-3.6865
Periodic (32)	-2.2202	-2.8374	-1.8499	-2.3006	-3.1895	-1.9111	-2.4222	-2.9930	-2.1848
Periodic (16)	-1.7182	-2.5124	-1.4694	-1.8482	-2.5931	-1.5708	-2.3323	-2.7434	-2.0008

IV. DISCUSSION AND CONCLUSION

In this study, the triangle pattern was used to reduce the receiving channels by applying the transmit-receive symmetry equations. Other methods to choose the receiving channels might also give similar performance. We used the triangle pattern because it can provide a simple and fast way to recover the traditional STA data.

There are some artifacts in the hypo-echoic lesions when they are placed near the probe. This is because when the two or four adjacent elements are combined, the array pitch will be increased to more than half a wavelength, and the grating-lobe artifacts will affect the image qualities, especially at large transmit/receive angles.

In conclusion, a new Hadamard-encoded STA approach with reduced receiving channels method is presented in this paper. The transmit-receive symmetry property can be effectively utilized to reduce the number of receiving channels by half without compromising the image qualities. Furthermore, schemes to encode the receiving elements can result in further reduction in the number of receiving channels and compensate partially for the degradation in image qualities in periodic sparse arrays. Therefore, the cost of an imaging system can be decreased due to the fewer electronics associated with the reduced number of active receiving channels. Although the initial simulations were implemented in 2D STA, this method can be extended to 3D STA imaging system.

V. ACKNOWLEDGMENT

The authors would like to thank the following funding agencies: Natural Sciences and Engineering Research Council of Canada (NSERC), the Canada Foundation for Innovation (CFI) and Ryerson University.

REFERENCES

- [1] R. Y. Chiao, L. J. Thomas and S. D. Silverstein, "Sparse array imaging with spatially-encoded transmits," in *Ultrasonics Symposium, 1997. Proceedings., IEEE*, 1997, pp. 1679-1682 vol.2.
- [2] P. Gong, A. Moghimi, M. C. Kolios, Y. Xu, "Delay-encoded Transmission in Synthetic Transmit Aperture (DE-STA) Imaging," *IEEE International Ultrasonics Symposium (IUS)*, 2014.
- [3] J. A. Jensen, S. I. Nikolov, K. L. Gammelmark and M. H. Pedersen, "Synthetic aperture ultrasound imaging," *Ultrasonics*, vol. 44, Supplement, pp. e5-e15, 12/22, 2006.
- [4] G. R. Lockwood, J.R. Talman, S.S. Brunke, "Real-time 3-D ultrasound imaging using sparse synthetic aperture beamforming," *IEEE Trans. Ultrason. Ferroelec. Freq. Contr.* 45 (1998) 980-988
- [5] G. R. Lockwood, P. C. Li, M. O'Donnell, and F. S. Foster, "Optimizing the radiation pattern of sparse periodic linear arrays," *IEEE Trans. Ultrason., Ferroelect., Freq. Contr.*, vol. 43, pp.7-14, 1996.
- [6] D. H. Turnbull et F. S. Foster, "Beam steering with pulsed two dimensional transducer arrays," *Ultrasonics, Ferroelectrics and Frequency Control*, IEEE Transactions on, vol. 38, no. 4, p. 320±333, 1991.
- [7] R. E. Davidsen, J. A. Jensen, and S. W. Smith, "Two-dimensional random arrays for real-time volumetric imaging," *Ultrason. Imag.*, vol. 16, pp. 143-163, 1994.
- [8] J. L. Schwartz and B. D. Steinberg, "Ultra sparse, ultra wide band arrays," *IEEE Trans. Ultrason., Ferroelect., Freq. Contr.*, vol. 45, no. 2, pp. 376-393, Mar. 1998
- [9] S. I. Nikolov and J. A. Jensen, "Application of different spatial sampling patterns for sparse array transducer design," *Ultrasonics*, vol. 37, no. 10, pp. 667-671, 2000
- [10] J. T. Yen, J. P. Steinberg, and S. W. Smith, "Sparse 2-D array design for real time rectilinear volumetric imaging," *IEEE Trans. Ultrason., Ferroelect., Freq. Contr.*, vol. 47, no. 1, pp. 93-110, Jan. 2000.
- [11] A. Austeng and S. Holm, "Sparse 2-D arrays for 3-D phased array imaging-Design methods," *IEEE Trans. Ultrason., Ferroelect., Freq. Contr.*, vol. 49, no. 8, pp. 1073-1086, Aug. 2002.
- [12] B. Diarra, M. Robini, P. Tortoli, C. Cachard, and H. Liebgott, "Design of Optimal 2-D Nongrid Sparse Arrays for Medical Ultrasound" *IEEE Transactions on Biomedical Engineering*, vol. 60, no. 11, Nov. 2013
- [13] M. Karaman, I. O. Wygant, Ö. Oralkan, and B. T. Khuri-Yakub, "Minimally Redundant 2-D Array Designs for 3-D Medical Ultrasound Imaging," *IEEE TRANSACTIONS ON MEDICAL IMAGING*, VOL. 28, NO. 7, JULY 2009
- [14] T. K. Moon and W. C. Stirling, "Mathematical Methods and Algorithms for Signal Processing," Upper Saddle, NJ:Prentice Hall, 2000
- [15] J. A. Jensen, "Field: A program for simulating ultrasound systems," *Med. Biol. Eng. Co River mput.*, vol. 34, pp. 351-353, 1996